

## Facile Synthesis of Crystalline SnO<sub>2</sub> Nanowires on Various Current Collector Substrates

Yu Zhong,<sup>a</sup> Yong Zhang,<sup>a</sup> Ruying Li,<sup>a</sup> Mei Cai<sup>b</sup> and Xueliang Sun<sup>a\*</sup><sup>a</sup>Department of Mechanical and Materials Engineering, University of Western Ontario, London, Ontario, N6A 5B9, Canada<sup>b</sup>General Motors Research and Development Center, Warren, Michigan 48090-9055

(Received: Apr. 18, 2012; Accepted: Jul. 9, 2012; Published Online: Sept. 3, 2012; DOI: 10.1002/jccs.201200220)

Crystalline SnO<sub>2</sub> nanowires with smooth surface and uniform diameter were readily produced via chemical vapor deposition (CVD) method on various current collectors including carbon paper, stainless steel and copper. The growth followed a vapor-liquid-solid (VLS) mechanism employing a gold thin film as the catalyst. Morphology, composition and structure of the SnO<sub>2</sub> nanowires on different collectors were characterized by scanning electron microscopy (SEM), transmission electron microscopy (TEM), energy dispersive X-ray spectroscopy (EDS) and X-ray diffraction (XRD). Morphology results demonstrated that the growth of SnO<sub>2</sub> nanowires only occurred in a narrow temperature range, while the structure and composition information unveiled the correlation between the quality of the nanowires and the employed substrates. The unique architecture of SnO<sub>2</sub> nanowires directly growing on current collectors are expected to act as building blocks in producing various types of nanodevices, especially as anode materials for Li-ion batteries.

**Keywords:** SnO<sub>2</sub> nanowires; Current collectors; Chemical vapor deposition.

### INTRODUCTION

As a wide-band gap ( $E_g = 3.6$  eV, at 300 K) semiconducting material, SnO<sub>2</sub> has been extensively investigated due to their wide applications in producing gas sensors,<sup>1-3</sup> catalyst supports,<sup>4</sup> field emitters,<sup>5</sup> transistors<sup>6</sup> and transparent electrodes.<sup>7</sup> Because of their distinct physical and chemical properties compared to their bulk counterparts, one-dimensional SnO<sub>2</sub> nanowires with a high surface-to-volume ratio and unique structure, are considered as promising materials in manufacturing nanodevices and attract intensive research interest.

Up to now, SnO<sub>2</sub> nanowires have been synthesized in various methods, including chemical vapor deposition (CVD),<sup>8-26</sup> heat treatment,<sup>27-29</sup> hydrothermal,<sup>30</sup> laser<sup>31</sup> and template methods.<sup>32-34</sup> Meanwhile, different precursors have been explored as well yielding dense products, such as Sn, SnO and SnO<sub>2</sub> precursors. Sn powder is commonly used as the starting material due to the low melting point (231 °C).<sup>8-13</sup> SnO (melting point: 1080 °C) is another choice acting as an assistant Sn source during the synthesis.<sup>14-20</sup> Despite its high melting point (1630 °C), SnO<sub>2</sub> mixed with graphite is also used to supply Sn precursors to the growth of SnO<sub>2</sub> nanowires.<sup>21-26</sup> Depending on applications and synthesis methods, SnO<sub>2</sub> nanowires have been prepared on

different supporting substrates. Yang et al. produced SnO<sub>2</sub> wires on a Si substrate;<sup>12</sup> Chen et al. approached piled SnO<sub>2</sub> nanowires on alumina collectors;<sup>17</sup> Ma et al. carried out the synthesis of SnO<sub>2</sub> nanowires on a LaAlO<sub>3</sub> substrate.<sup>35</sup> Aiming at meeting the development requirements of device building blocks, dense SnO<sub>2</sub> nanowires with high quality should be explored on various potential substrates.

To apply SnO<sub>2</sub> nanowires as the building blocks in electronic devices such as anode materials of Li-ion battery, it is essential to provide a superior contact between the nanowires and current collectors. Directed by this motivation, the growth of SnO<sub>2</sub> nanowires has been carried out on different potential current collectors. In this work, we present the synthesis of dense SnO<sub>2</sub> nanowires in a simple CVD process on the potential current collectors including carbon paper, stainless steel and Cu. After reaction, dense products were obtained on these substrates and were characterized to reveal the details of the nanowires. A systematic investigation of the effects of temperature and substrates on the growth of SnO<sub>2</sub> nanowires was conducted.

### EXPERIMENTAL

SnO<sub>2</sub> nanowires were synthesized by the CVD method in a quartz tube mounted in a tube furnace as shown Figure

Special Issue for the Electrical Energy Storage and Conversion

\* Corresponding author. Tel: +1 519 661 2111 ext. 87759; Fax: +1 519 661 3020; E-mail: xsun@eng.uwo.ca

1. Pure Sn powder was used as the starting material and was placed in the center of the quartz tube. Carbon paper, stainless steel and Cu were chosen as the substrates for the growth of SnO<sub>2</sub> nanowires. The metallic substrates (stainless steel and Cu) were pre-treated by polishing with sand paper firstly, and then etched with HCl (1 mol/L) for 30 min. Finally, the metallic substrates were washed with distilled water and dried. After the pre-treatment, a thin Au layer with 5 nm in thickness was deposited on the surface of the metallic substrates by sputtering. Au film was directly deposited on carbon paper without any pre-treatment. The substrates were placed near Sn powder at the down stream of an Ar flow (400 sccm) which was used as carrier gas. Before the reaction started, the tube was purged by Ar flow for 15 min. Then the furnace was heated up to the required temperatures (780–790 °C) to trigger the growth of SnO<sub>2</sub> nanowires on the surface of substrates. The reaction last for 2 hours. Finally, the furnace was turned off and cooled down to the room temperature.

The products were characterized by using field emission scanning electron microscopy (FE-SEM, Hitachi 4800S SEM), transmission electron microscopy (TEM, Hitachi 7000), energy dispersive X-ray spectroscopy (EDS) and X-ray diffraction (XRD, Rigaku Co K $\alpha$  radiation).

## RESULTS AND DISCUSSION

### Carbon paper substrate

Figure 2a–c show the characterization results of the products growing on the carbon paper substrate at 780 °C, 785 °C and 790 °C, respectively. At 780 °C, dense particles with diameter around 50 nm were deposited on the surface of carbon fibers (Figure 2a). When the temperature was increased to 785 °C, high yield nanowires were observed on the surface of carbon fibers (Figure 2b). However, as the temperature was further increased to 790 °C, these nanowires disappeared and the surface of carbon fibers was covered by particles with the similar size of that was observed

at 780 °C (Figure 2c). That indicates the growth of these SnO<sub>2</sub> nanowires is quite sensitive to the reaction temperature. The growth occurs in a very narrow temperature range, and the growth of nanowires is terminated beyond the temperature range.

After reaction at 785 °C, the obtained SnO<sub>2</sub> nanowires are very dense. Seen from the high magnification SEM image (Figure 2b insert), diameter of the SnO<sub>2</sub> nanowires ranges from 40 to 80 nm. The surface of the nanowires is smooth and clean without any impurity particles. More detailed observation of the nanowires shown in the TEM image (Figure 2d) indicates that the nanowires are very straight and possess a smooth surface. Some of the nanowires are also entangled with each other due to van der Waals interactions. Particles are found at the tips of the nanowires in SEM images (Figure 2b insert and f), which indicates the growth of these SnO<sub>2</sub> nanowires follows a vapor-liquid-solid (VLS) process.<sup>8,10,13</sup>

In the VLS process, Au particles firstly form on the surface of the substrate acting as catalyst for the growth of nanowires.<sup>8,10,23</sup> Sn is vaporized from the starting material and transported by the Ar flow to the reaction zone. The vaporized Sn precursors collected by the Au particles would diffuse along the surface of Au particles and Sn-Au liquid alloy can form. Due to the presence of residue oxygen inside the system, the oxygen reacts with the Sn-Au alloy to

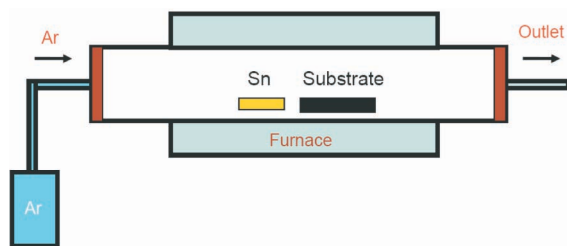


Fig. 1. Schematic diagram of the equipment setup of CVD process.

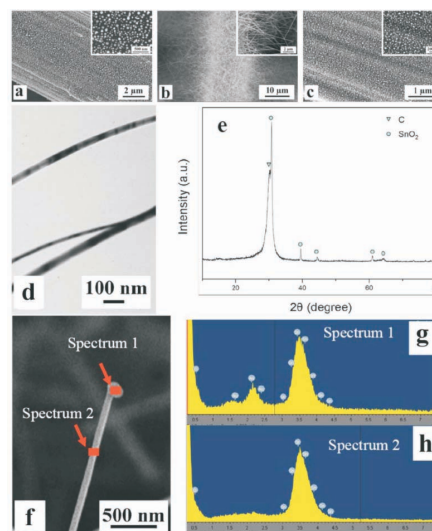


Fig. 2. SEM images of products on carbon paper at different temperatures: a) 780 °C, b) 785 °C and c) 790 °C; d) TEM image of SnO<sub>2</sub> nanowires synthesized at 785 °C; e) XRD patterns of products synthesized at 785 °C; f–h) EDS results of individual SnO<sub>2</sub> nanowire.

form SnO<sub>2</sub> and precipitate from the alloyed particles.<sup>10</sup> Directed by the Sn-Au alloyed particles, SnO<sub>2</sub> nanowires are finally obtained.

Figure 2e shows the XRD patterns of SnO<sub>2</sub> nanowires. In Figure 2e, peaks at 31.0, 39.5, 44.3 and 64.5° are perfectly matched with that of a tetragonal rutile SnO<sub>2</sub> structure (JCPDS card No. 41-1445). The sharp and strong peaks suggest high crystallinity of the SnO<sub>2</sub> nanowires. The peak at 30.7° is indexed to graphite (JCPDS card No. 41-1487) which comes from the carbon substrate. No peaks of residual Sn and other impurities are found.

Composition information of the individual SnO<sub>2</sub> nanowires is characterized by EDS spectra as shown in Figure 2f-h. Strong peaks of Sn (23.10 at%), O (74.16 at%) and Au (2.74 at%) elements are observed in EDS spectrum 1 (Figure 2g) being taken at the particle supported at the tip of nanowire. In terms of spectrum 2 (Figure 2h) taken at the body of the nanowire, only Sn (22.75 at%) and O (77.25 at%) element peaks are observed. That means the growth of SnO<sub>2</sub> nanowires is directed by Au catalyst and follows a tip-growth VLS mechanism.

#### Stainless steel substrate

The synthesis of SnO<sub>2</sub> nanowires on stainless steel substrate followed the similar procedures to that used for producing SnO<sub>2</sub> nanowires on carbon paper. According to the above results, it is known that the growth of SnO<sub>2</sub> nanowires is quite sensitive to the experimental conditions, especially the growth temperature. Hence the synthesis of SnO<sub>2</sub> nanowires on the stainless steel substrate was investigated in a narrow temperature range from 780 °C to 790 °C as well.

Figure 3a-c show the SEM analysis of the products synthesized at different temperatures: 780 °C, 785 °C and 790 °C. At the temperature of 780 °C, the surface of the substrate was covered by a lot of particles (Figure 3a). Among the particles, some tiny nanoflakes with vary thin thickness about 10 nm are observed (Figure 3a insert). When the reaction temperature was increased to 785 °C, dense products with nanowire-like morphology were obtained on the surface of the stainless steel substrate (Figure 3b). It can be seen that the nanowires exhibit bundle-like structure (Figure 3b insert) and each bundle is composed of several individual nanowires. These nanowires possess the smooth and clean surface. The diameter of the nanowires ranges from 80 to 200 nm. The TEM image (Figure 3d) reveals straight shape and very clean surface of the SnO<sub>2</sub> nanowires. Tiny Au particles are clearly observed at the

tips of nanowires in the TEM image which provides strong evidence accounting for the VLS mechanism that the nanowire growth followed. As temperature was further increased to 790 °C, the substrate was covered by a large amount of particles again (Figure 3c). Some very thin nanowalls of 30 nm in thickness were also found among the big particles (Figure 3c insert). The results from different reaction temperatures reveal that the growth of SnO<sub>2</sub> on stainless steel substrate also strongly depends on the growth temperature. Dense nanowires can only be obtained around at 785 °C. Beyond this optimal temperature, the stainless steel is mainly decorated by dispersed particles on the surface.

Figure 3e shows the XRD patterns of the nanowires growing on stainless steel substrate at 785 °C. The peaks are well indexed to SnO<sub>2</sub> at 31.0, 39.5 and 60.9° (JCPDS card No. 41-1445), which confirms the phase structure of the as-synthesized products as SnO<sub>2</sub> nanowires. Some signals of FeNi<sup>3</sup> (JCPDS card No. 38-0419) and Co (JCPDS card No. 05-0727) mainly arise from the substrate.

Because the stainless steel contains various elements like Fe, Ni and Cr, which may affect the growth of SnO<sub>2</sub> nanowires, EDS was carried out to analyze the composition of nanostructures (Figure 3f-h). Spectrum 1 (Figure 3g) exhibits the signals of the particle supported at the tip of the individual nanowire. Peaks of Sn (7.90 at%), O (63.18

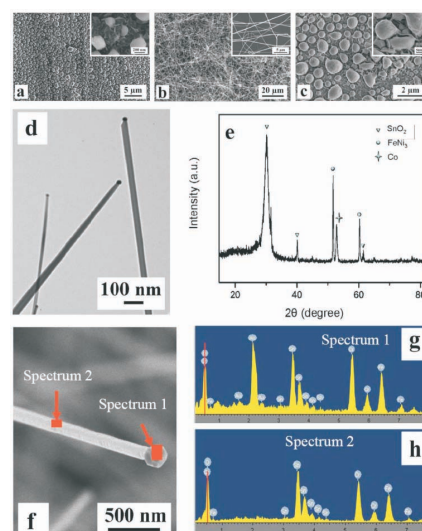


Fig. 3. SEM images of products on stainless steel at different temperatures: a) 780 °C, b) 785 °C and c) 790 °C; d) TEM image of SnO<sub>2</sub> nanowires synthesized at 785 °C; e) XRD patterns of products synthesized at 785 °C; f-h) EDS results of individual SnO<sub>2</sub> nanowire.

at%), Au (4.93 at%), Fe (10.97 at%) and Cr (13.02 at%) are shown in spectrum 1. Au signal is quite strong which demonstrates the particle is Au-rich to direct the growth of nanowires following VLS process. Detection of Fe and Cr signals also indicates that elements may be dissolved into the particle. Spectrum 2 (Figure 3h) shows the information of the body of the individual nanowire. In spectrum 2, Sn (7.33 at%) and O (73.12 at%) elements show dominant peaks, while Fe (8.82 at%) and Cr (10.73 at%) signals are captured as well, which means the nanowires are tin oxide nanowired doped with Fe and Cr elements.

### Cu substrate

The synthesis procedures of SnO<sub>2</sub> nanowires on Cu substrate are the same with that of stainless steel. Because of the sensitivity of the growth, the reaction temperature range was also conducted from 780 °C to 790 °C.

Figure 4a-c show the characterization results on the Cu substrate at the reaction temperature of 780 °C, 785 °C and 790 °C, respectively. In the case of 780 °C, Figure 4a shows that the Cu substrate is covered by a large amount of particles with irregular shape and large diameter. The particles distribute through the whole substrate. Due to the temperature sensitivity of the growth of SnO<sub>2</sub> nanowires, temperature was increased by 5 °C to 785 °C which was used as the optimal temperature for the growth of SnO<sub>2</sub> nanowires on carbon paper and stainless steel. After reaction, high

yield of SnO<sub>2</sub> nanowires was achieved on the substrate (Figure 4b). Quite similar to the nanowires growing on stainless steel, the products on Cu have the bundle-like structure. Each bundle consists of several individual nanowires (Figure 4b insert). The nanowires are straight and thin, with diameter ranging from 40 to 200 nm. TEM image in Figure 4d also shows the structure information of the SnO<sub>2</sub> nanowires. These nanowires possess a straight shape and the surface is quite smooth and clean. The results are consistent with SEM analysis above. When the reaction temperature was increased to 790 °C, particles with irregular shape were the only deposition products on the substrate surface (Figure 4c). The results are quite similar to that obtained at 780 °C, and indicate that the temperature has moved out the optimal temperature range of the growth of SnO<sub>2</sub> nanowires.

XRD patterns of the SnO<sub>2</sub> nanowires growing on Cu substrate are shown in Figure 4e. Main signals come from the nanowires and Cu substrate. XRD patterns clearly show that the signals originate from SnO<sub>2</sub> nanowires at 31.0, 39.5, 44.3, 60.9, 64.5, 68.3, 74.1, 76.8 and 78.4° (JCPDS card No. 41-1445). Cu peaks from the substrate at 50.7 and 59.3° (JCPDS card No. 04-0836) are also detected.

Particles are also found at the tips of nanowires (Figure 4f), which indicate the same VLS growth mechanism of the nanowires as that on carbon paper and stainless steel substrates. EDS spectra are presented to provide the information of particles supported at the tip and body of the individual nanowire. Spectrum 1 shows the composition information of the particle at the tip (Figure 4g). In spectrum 1, Sn (14.00 at%), O (58.10 at%), Au (0.47 at%) and Cu (27.43 at%) peaks are observed. Au signals deriving from the particle, reveal that the growth mechanism should follow the VLS process assisted by Au catalyst. Cu signals indicate that Cu was partially dissolved into the particle. In spectrum 2 (Figure 4h), the strong peaks of Sn (22.39 at%) and O (74.02 at%) are detected and weak peaks of Cu (3.59 at%) are also observed. That indicates Cu was incorporated into the nanowires.

From the above results, it can be seen clearly that the synthesis temperature and surface condition of substrates play crucial roles in affecting the growth of SnO<sub>2</sub> nanowires. In spite of the employed substrates, the growth of SnO<sub>2</sub> nanowires can only occur in a very narrow temperature range which indicates the sensitive growth of the nanowires subjecting to temperature. The reason may arise from the influence of temperature on the degree of supersatura-

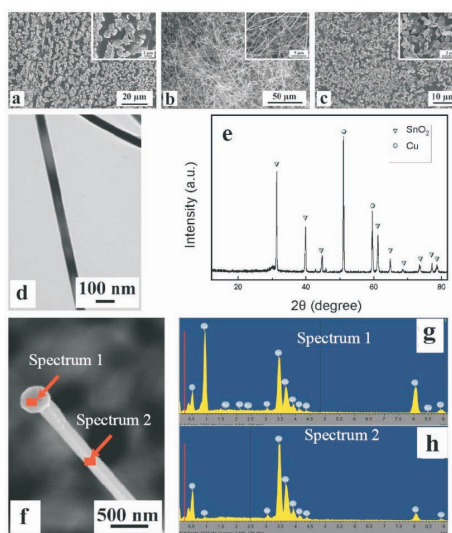


Fig. 4. SEM images of products on Cu at different temperatures: a) 780 °C, b) 785 °C and c) 790 °C; d) TEM image of SnO<sub>2</sub> nanowires synthesized at 785 °C; e) XRD patterns of products synthesized at 785 °C; f-h) EDS results of individual SnO<sub>2</sub> nanowire.

tion of Sn precursor and partial pressure of oxygen in the reaction zone. Based on our experimental results, certain degree of saturation of Sn precursor and partial pressure of oxygen are critical prerequisite for anisotropic growth of the nanowires. At relatively lower temperature (780 °C), low concentration of Sn vapour is not able to trigger the growth of nanowires. However, if the temperature is relatively higher (790 °C), high degree of saturation of Sn precursor may restrict the diffusion of oxygen resulting in too low partial pressure of oxygen in the reaction zone, which also inhibits the growth of the nanowires. Only at the optimal temperature (785 °C), the reaction conditions could be balanced at the proper level for the oriented growth of nanowires.

On the other hand, morphology and size difference of the nanowires on different substrates also unveil the fact that the surface condition of substrates can affect the growth of the SnO<sub>2</sub> nanowires. Due to the inert surface condition of carbon paper, the Au catalyst may direct the growth of nanowires without any interruption, and the body of nanowires was characterized as pure SnO<sub>2</sub>. However, the growth circumstance is quite different on the stainless steel and Cu from carbon paper. Although Au is still rich in the particles at the tips of nanowires growing on the metallic substrates, other elements like Fe, Cr and Cu are also detected on both tip and body of the nanowires. The reason can be interpreted from the perspectives of surface condition of the metallic substrates. The pre-treatment may remove the contaminant at the surface of metallic substrates, and also makes the surface condition active. When Sn-Au liquid alloyed particles form on the substrates, the metal elements (Fe, Cr, Cu) on the active surface can be easily dissolved into the liquid particles and the triple or multi-component catalyst may form, which would inevitably influence the catalytic effect of Au on the growth of nanowires. In the VLS growth process, diameter of the nanowires is determined by the size of the catalyst particles. With the assistance of pure Au, the SnO<sub>2</sub> nanowire is very thin with diameter ranging from 40 to 80 nm. When the catalyst particles are alloyed by elements from metal substrates, the involvement of these elements creates the triple or multi-component catalyst particles, thereby affects the nucleation and growth of the nanowires thermodynamically and kinetically, and finally influences the diameter of the obtained nanowires. On the other hand, the involved substrate elements also precipitate along the SnO<sub>2</sub> nanowires from the catalyst particles and locate along the axis of

the growth direction of the nanowires, which generates Fe, Cr and Cu doped SnO<sub>2</sub> nanowires. Further work is underway to investigate the performance of pristine and doped SnO<sub>2</sub> nanowires along with the current collectors on the lithium ion battery applications and the influence of doped element species and content on the size and structure of the SnO<sub>2</sub> nanowires as well.

## CONCLUSIONS

SnO<sub>2</sub> nanowires have been obtained on various substrates: carbon paper, stainless steel and Cu. To obtain SnO<sub>2</sub> nanowires, different reaction temperatures were conducted from 780 °C to 790 °C. The growth of SnO<sub>2</sub> nanowires is quite temperature-dependent. Dense SnO<sub>2</sub> nanowires were only obtained in a narrow temperature range around 785 °C. The SnO<sub>2</sub> nanowires are long and thin with very clean and smooth surface. The growth of nanowires followed a VLS process. The trace of Fe, Cr and Cu are also detected in the nanowires synthesized on stainless steel and Cu substrates. The unique SnO<sub>2</sub> nanowires directly growing on the current collectors can be used as building blocks in many potential applications, especially as anode materials for Li-ion batteries.

## ACKNOWLEDGEMENTS

This research was supported by National Science and Engineering Research Council (NSERC), General Motors of Canada, Canada Research Chair (CRC) program, Canadian Foundation for Innovation (CFI), and the University of Western Ontario.

## REFERENCES

1. Anasari, S. G.; Boroojerdian, P.; Sainkar, S. R.; Karekar, R. N.; Aiyer, R. C.; Kulkarni, S. K. *Thin Solid Films* **1997**, *295*, 271.
2. Wang, Y.; Jiang, X.; Xia, Y. *J. Am. Chem. Soc.* **2003**, *125*, 176.
3. Kolmakov, A.; Zhang, Y. X.; Cheng, G. S.; Moskovits, M. *Adv. Mater.* **2003**, *15*, 997.
4. Dazhi, W.; Shulin, W.; Jun, C.; Suyuan, Z.; Fangqing, L. *Phys. Rev. B* **1994**, *49*, 282.
5. Chen, Y. J.; Li, Q. H.; Liang, Y. X.; Wang, T. H.; Zhao, Q.; Yu, D. P. *Appl. Phys. Lett.* **2004**, *85*, 5682.
6. Cheng, Y.; Xiong, P.; Field, L.; Zheng, J. P.; Yang, R. S.; Wang, Z. L. *Appl. Phys. Lett.* **2006**, *89*, 093114.
7. He, Y. S.; Campbell, J. C.; Murphy, R. C.; Arendt, M. F.; Swinnea, J. S. *J. Mater. Res.* **1993**, *8*, 3131.
8. Yu, F.; Tang, D.; Hai, K.; Luo, Z.; Chen, Y.; He, X.; Peng, Y.; Yuan, H.; Zhao, D.; Yang, Y. *J. Cryst. Growth* **2010**, *312*,

- 220.
9. Park, S.; Hong, C.; Kang, J.; Cho, N.; Lee, C. *Curr. Appl. Phys.* **2009**, *9*, s230.
10. Yin, W.; Wei, B.; Hu, C. *Chem. Phys. Lett.* **2009**, *471*, 11.
11. Ra, H.-W.; Kim, K. J.; Im, Y. H. *Superlattice. Microst.* **2008**, *44*, 728.
12. Yang, M.-R.; Chu, S. Y.; Chang, R.-C. *Sens. Actuators B* **2007**, *122*, 269.
13. Kim, H. W.; Shim, S. H. *J. Korean Phys. Soc.* **2005**, *47*, 516.
14. Thanasanvorakun, S.; Mangkorntong, P.; Choopun, S.; Mangkorntong, N. *Ceram. Int.* **2008**, *34*, 1127.
15. Calestani, D.; Zha, M.; Salviati, G.; Lazzarini, L.; Zanotti, L.; Comini, E.; Sberveglieri, G. *J. Cryst. Growth* **2005**, *275*, e2083.
16. Thong, L. V.; Hoa, N. D.; Le, D. T. T.; Viet, D. T.; Tam, P. D.; Le, A. T.; Hieu, N. V. *Sens. Actuators B* **2010**, *146*, 361.
17. Chen, Y. X.; Campbell, L. J.; Zhou, W. L. *J. Cryst. Growth* **2004**, *270*, 505.
18. Calestani, D.; Zha, A. Z. M.; Lazzarini, L.; Salviati, G.; Zanotti, L.; Sberveglieri, G. *Mater. Sci. Eng., C* **2005**, *25*, 625.
19. Leonardy, A.; Hung, W. Z.; Tsai, D. S.; Chou, C. C.; Huang, Y. S. *Cryst. Growth Des.* **2009**, *9*, 3958.
20. Li, P. G.; Guo, X.; Wang, X. F.; Tang, W. H. *J. Alloys Compd.* **2009**, *479*, 74.
21. Kock, A.; Tischner, A.; Maier, T.; Kast, M.; Edtmaier, C.; Gspan, C.; Kothleitner, G. *Sens. Actuators, B* **2009**, *138*, 160.
22. Li, P. G.; Lei, M.; Tang, W. H.; Guo, X.; Wang, X. *J. Alloys Compd.* **2009**, *477*, 515.
23. Budak, S.; Miao, G. X.; Ozdemir, M.; Chetry, K. B.; Gupta, A. *J. Cryst. Growth* **2006**, *291*, 405.
24. Li, P. G.; Lei, M.; Wang, X.; Tang, W. H. *Mater. Lett.* **2009**, *63*, 357.
25. Lee, J.-S.; Sim, S. K.; Min, B.; Cho, K.; Kim, S. W.; Kim, S. *J. Cryst. Growth* **2004**, *267*, 145.
26. Li, L.; Zong, F.; Cui, X.; Ma, H.; Wu, X.; Zhang, Q.; Wang, Y.; Yang, F.; Zhao, J. *Mater. Lett.* **2007**, *61*, 4152.
27. Ahn, J.-H.; Kim, Y. J.; Wang, G. *J. Alloys Compd.* **2009**, *483*, 422.
28. Wang, W. Z.; Niu, J.; Ao, L. *J. Cryst. Growth* **2008**, *310*, 351.
29. Chen, M.; Xia, X.; Wang, Z.; Li, Y.; Li, J.; Gu, C. *Microelectron. Eng.* **2008**, *85*, 1397.
30. Lupan, O.; Chow, L.; Chai, G.; Schulte, A.; Park, S.; Heinrich, H. *Mater. Sci. Eng., B* **2009**, *157*, 101.
31. Chen, Z. W.; Jiao, Z.; Wu, M. H.; Shek, C. H.; Wu, C. M. L.; Lai, J. A. L. *Mater. Chem. Phys.* **2009**, *115*, 660.
32. Zheng, M.; Li, G.; Zhang, X.; Huang, S.; Lei, Y.; Zhang, L. *Chem. Mater.* **2001**, *13*, 3859.
33. Kim, H.; Cho, J. *J. Mater. Chem.* **2008**, *18*, 771.
34. Qu, D. M.; Yan, P. X.; Chang, J. B.; Yan, D.; Liu, J. Z.; Yue, G. H.; Zhou, R. F.; Feng, H. T. *Mater. Lett.* **2007**, *61*, 2255.
35. Ma, Y.; Zhou, F.; Lu, L.; Zhang, Z. *Solid State Commun.* **2004**, *130*, 313.